

Interferometer instrument design for New Millennium Deep Space 3

G. H. Blackwood, S. Dubovitsky, R. P. Linfield, and P. W. Gorham

Jet Propulsion Laboratory

California Institute of Technology

4800 Oak Grove Drive, Pasadena, CA 91109

ABSTRACT

Deep Space 3 will fly a stellar optical interferometer on three separate spacecraft in heliocentric orbit: one spacecraft for the Michelson beam combining optics, and two spacecraft for each of the starlight apertures. The spacecraft will formation fly to relative spacecraft distances from 100 meters to 1 kilometer, enabling an instrument resolution of 1 to 0.1 milliarcsecond. At each baseline length and orientation—up to 100 points in the synthetic aperture plane for a given astrophysical target—the instrument will measure source visibility amplitude from which the source brightness distribution can be determined. An infrared metrology system performs both linear and angular metrology between spacecraft and is used to estimate delay jitter, interferometer delay and delay rate. Pointing and control mechanisms use the metrology error signals to stabilize delay jitter and to null delay and delay rate to enable detection and tracking of a white light fringe on a photon-counting detector. Once stabilized, fringes can be dispersed on a CCD in up to 80 spectral channels to attain high-accuracy measurements of visibility amplitude as a function of wavelength.

Keywords: space-based optical interferometry, formation flying, metrology, active optics, Michelson interferometer

1. INTRODUCTION

Deep Space 3 (DS3), the third mission in the New Millennium Program, will validate advanced technologies for future spacecraft and instruments. Among these technologies are deep space formation flying of multiple spacecraft—to accuracies in relative range and attitude of 1 cm and 1 arcmin, respectively—and the demonstration of space-based Michelson interferometry in visible wavelengths at short (2-m) and long (100-m to 1-km) baselines. Separated spacecraft optical interferometry is an enabling technology for Terrestrial Planet Finder, a 100-m infrared interferometer mission in the ORIGINS roadmap,¹ one that may be implemented on separate spacecraft. DS3 also builds confidence for the Space Interferometry Mission (SIM)² by validating a significant amount of common software and hardware elements required for the instrument subsystems.

Figure 1 illustrates the DS3 mission configuration. Two collector spacecraft, at the base of the triangle, establish the interferometer baseline perpendicular to the line of sight to the astrophysical target. The combiner spacecraft is at the apex. One aperture (13-cm flat siderostat) on each of the two collectors directs starlight to the combiner spacecraft, where the beams are combined at a beamsplitter to produce interference fringes; the fringe modulus is the science observable. The fringe modulus is measured at different baselines and baseline orientations—achieved by scaling the collector-collector distance and by rotating the baseline about the line of sight.

DS3 is to be launched in 2002 on a Delta 2 rocket into a heliocentric, Earth-trailing orbit as a single cluster of three connected spacecraft. The Earth-trailing orbit is attractive for its constant thermal environment and low disturbance torques. At the end of the 6-month mission the spacecraft will be 0.1 AU from the Earth. DS3 will first perform

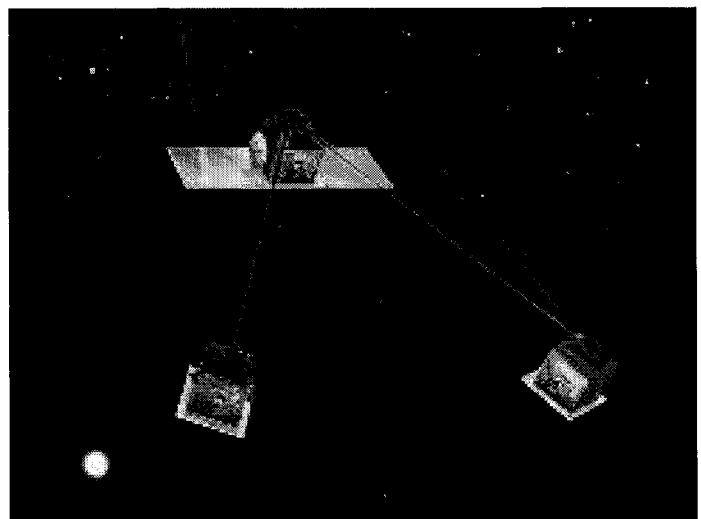


Figure 1: Mission concept for Deep Space 3. Infrared metrology links interferometer optics on three separate spacecraft.

Further author information:

Email: gary.blackwood@jpl.nasa.gov; Telephone 818-354-6263

optical interferometry in cluster mode on a fixed 2-m baseline; afterwards, the three spacecraft will separate and perform formation flying maneuvers. Finally, optical interferometry will be implemented between the spacecraft at baselines of 100 m to 1 km. The constellation geometry of an equilateral triangle, as illustrated in Figure 1, is not unique; other isosceles triangles are acceptable, including the limit of a linear array of equally spaced spacecraft. The normal to the constellation plane is maintained within 45° of the Sun direction to avoid thermal and light contamination of the instrument optics.

Because the DS3 orbit is well outside the Global Positioning System (GPS) constellation, spacecraft relative distances and relative attitudes will be measured on board by the Autonomous Formation Flying (AFF) sensor,³ a transceiver derived and developed from GPS tracking technology. The AFF uses multiple antennas on each spacecraft to transmit and receive radio-frequency ranging and carrier signals in the 30 GHz band. The AFF provides 4π steradian coverage and accuracies of ± 1 cm in and ± 1 arcmin in relative orientation. A star tracker on the combiner spacecraft measures inertial attitude to ~ 10 arcsec.

Spacecraft propulsion is provided by pulse plasma thrusters (PPTs) for both translational maneuvers and attitude control.^{4,5} PPTs operate at high specific impulse (1150 s) and generate impulses of 60 to 700 $\mu\text{N}\cdot\text{s}$, which when applied in pairs to a 150-kg spacecraft, impart a ΔV of between 0.8 and 9 $\mu\text{m/s}$. Formation flying control⁶ uses the AFF and combiner star tracker to command the PPTs and establish the instrument baseline at the prescribed length and attitude with respect to the optical target. The formation control also holds the constellation within the ~ 1 -arcmin tolerances necessary for the interspacecraft metrology to acquire and lock.

The masses of each spacecraft, including instruments, are 150 kg for each collector and 250 kg for the combiner. The instrument masses themselves are 25 kg for each collector and 77 kg for the combiner. Solar panels on each spacecraft provide 35 W for the collectors and 135 W for the combiner. The mission computer and mission executive are centralized on the combiner spacecraft, which coordinates all constellation and instrument functions through an interspacecraft communication link with a data rate of 1 Mbit/s.

The remainder of the paper describes the instrument architecture and the requirements imposed on the instrument subsystems.

2. INSTRUMENT ARCHITECTURE AND REQUIREMENTS

DS3 will fly a single-baseline Michelson interferometer similar in architecture to ground-based instruments.^{7,8} In a Michelson interferometer starlight is collected at two separated apertures, brought to a central beamsplitter where the light is combined, and then focused onto a single-pixel, photon-counting detector. When both the pathlength and wavefront tilt of each starlight leg are equal, an interference fringe will be created; the shape and amplitude of the interference fringe may be measured by varying the pathlength in one of the starlight paths.

Knowledge of the source fringe amplitude and phase for all baseline lengths and orientations throughout the synthetic aperture plane provides, in principle, complete knowledge of the two-dimensional Fourier transform of the object brightness distribution, from which the source image can be recovered by inversion.⁹ However, a single-baseline Michelson interferometer cannot determine the absolute fringe phase at each point in the aperture plane, due to the large uncertainty of the baseline orientation in inertial space (unless there is a bright unresolved source in the very narrow image field, or, as in SIM, the science baseline is referenced to inertial guide stars by two other interferometer baselines). DS3 can, in general, measure only fringe amplitudes throughout the synthetic aperture plane. Parameter fitting or iterative inversion techniques can be used to extract information about the source brightness distribution based only on fringe amplitudes.

2.1 Science

At baselines of $B = 1000$ km the resolution of the interferometer will be $\lambda/B = 100$ μarcsec at visible wavelength $\lambda = 550$ nm. At the planned limiting magnitude of $V = 12$, DS3 will reach baselines and magnitudes not currently accessible to ground-based interferometers (currently operating at baselines of ~ 100 m and 5th-to-8th magnitude). DS3 will be able to investigate the structure of X-ray binaries, the outflow structure of Wolf-Rayet stars, the diameter of hot (O and B) stars, and stellar limb darkening. Figure 2 illustrates the parameter space (visual brightness vs baseline length) that would be expected for DS3.¹⁰ Magnitudes are limited to $V=12$ at long baselines by instrumental effects: Uncertainty in the interferometer delay rate knowledge limits the fringe search speed for dim stars. Baselines, however, are limited by physics: The fringes of bright stars cannot be detected at long baselines. Because of their proximity, the disks of bright stars subtend angles comparable to or larger than the interferometer resolution; fringes for these stars can be detected by reducing the interferometer baseline. At

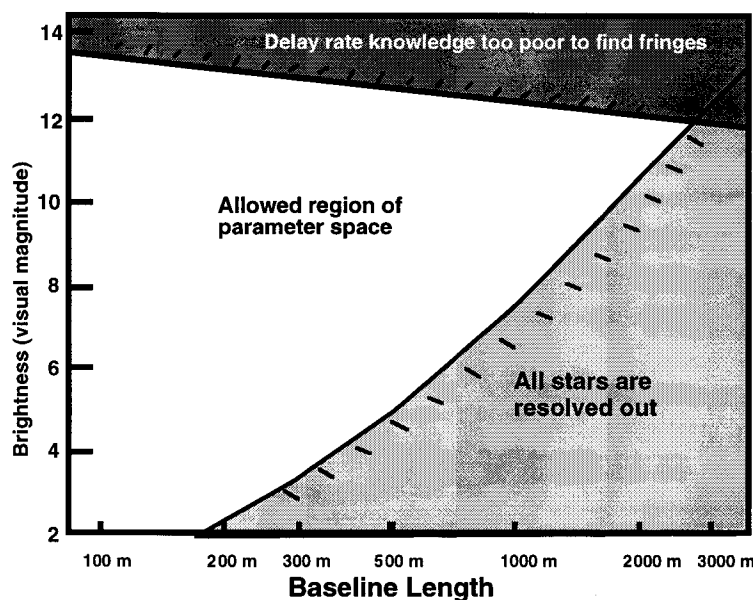


Figure 2: Observation parameter space for Deep Space 3.

the longest baselines the interferometer must limit fringe searching to fainter stars—whose greater distances imply smaller angular sizes.

2.2 Fundamental instrument requirements

Table 1 lists the fundamental instrument requirements. DS3 will observe at visible wavelengths on baselines of 2 m (during checkout in cluster mode on bright stars) and observe sources of 12th magnitude on baselines of 100 m to 1 km when the spacecraft are separated. Source fringe visibilities are to be measured to an accuracy of 1% of unit visibility, or to an accuracy of 0.01, in up to 80 spectral channels in the optical bandpass. Fringe visibility is a measure of the fringe amplitude; it is 1 for an unresolved point source and decreases toward zero as the angle subtended by the source increases. Each baseline vector must be known to 1-m accuracy for purposes of image reconstruction. This accuracy level is easily met by the constellation AFF sensor.

Three levels of synthetic aperture plane coverage are assumed as an observing plan.¹¹ The first, 1-D coverage, consists of measurements every 100 m in separation in one direction, from 100 m to 1 km. The second and third levels—limited and full aperture plane coverage—are illustrated in Figure 3. The solid line represents the aperture plane coverage at one epoch, and the dashed line represents the coverage 3 months later when the Sun-source angle has changed. The coverages in Figure 3 are possible for sources near the ecliptic poles, given the mission requirement that the normal to the constellation plane be maintained to within 45° of the Sun direction; more limited coverage is available for other regions of the celestial sphere. Over the course of 3 months any source in the celestial sphere can receive 1-D coverage.

Table 1: Instrument Requirements

Parameter	Requirement
Baseline	100 m to 1 km, variable 2 m (connected structure)
Wavelength	400 to 1000 nm
Observable	Fringe visibilities, calibrated to 1%
Limiting Magnitude	12
Aperture Plane Coverage	60 stars, 10 u-v points 30 stars, 40 u-v points 10 stars, 100 u-v points
Aperture Plane Position Accuracy	1 m

2.3 Requirement flowdown

Spacecraft maneuvers are required to change the baseline length or orientation. At each measurement point in the synthetic aperture plane it is assumed that the relative spacecraft velocities are brought to zero—termed the ‘stop and stare’ mode of operation. These functions generate requirements for the design of the instrument subsystems described in Section 3.

Acquire interspacecraft metrology: The AFF sensor will provide knowledge of the interspacecraft relative angles to ± 1 arcmin; at 1 km, ± 1 arcmin corresponds to ± 30 cm. Three metrology beams (between each of three pairs of spacecraft) must be steered over this range, be intercepted by detectors on the opposing spacecraft, and then be reflected to the spacecraft from which the beams originated. Metrology acquisition requires pointing accuracy to ~ 1 arcsec.

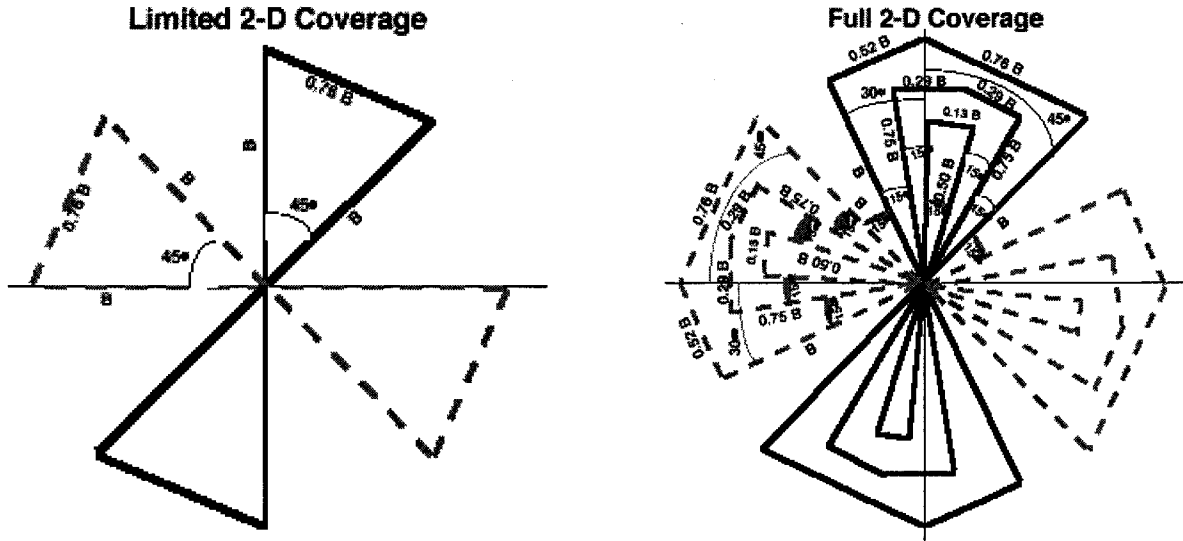


Figure 3: Examples of limited and full 2-D coverage of the synthetic aperture plane.

Acquire starlight on the detectors: Using inertial attitude knowledge from a star tracker on the combiner spacecraft, along with interspacecraft angular metrology knowledge, the collector apertures must be pointed such that starlight beam is incident to the combiner optics. This function requires a starlight pointing accuracy of ~ 4 cm of shear error, or equivalently, an accuracy of a ~ 8 arcsec at 1 km.

Estimate interferometer delay: In order to find fringes with DS3, it will be necessary to estimate the interferometer delay¹²—defined by the difference in starlight pathlengths in each arm of the interferometer, measured from a common incoming planar wavefront, reflected off the collector apertures and finally incident to the beamsplitter on the combiner spacecraft. The delay contains contributions from internal constellation deformations as well as a contribution from an overall inertial in-plane constellation rotation. Figure 4 illustrates the geometry of this inertial rotation, in which the spacecraft attitudes, interspacecraft distances and included interspacecraft angles θ_i all remain fixed, but in which the source-baseline angle θ_s has changed. To determine this rotation angle—and thus the delay—linear metrology is insufficient; it will be necessary to measure the baseline length and to measure metrology and starlight angles. The length of time needed to find fringes will be proportional to the delay uncertainty. To limit search times for dim (12th-magnitude) sources, the delay must be estimated to within 2 mm. This delay results in a 2000-s fringe search time (assuming a delay search speed of $1 \mu\text{m/s}$, given a delay window of $1 \mu\text{m}$ and a dim star coherence time of ~ 1 s).

Estimate and null delay rate: The time rate of change of the delay—due to both internal deformations and an inertial in-plane angular rotation of the constellation—must be known to the level of the fringe search speed, or to $1 \mu\text{m/s}$, in order for the fringes to be detectable during the search. No spacecraft translational thruster firings are permitted during delay rate estimation or fringe searching. This estimate is made from the time rate of change of laser and starlight angles, plus length changes as measured by the laser metrology.

Search for and track the starlight fringe: The starlight (optical) delay is scanned throughout the interferometer delay uncertainty range by an optical delay line; photons are counted at a single-pixel detector after the beams are combined at a beamsplitter. One possible fringe search method involves synchronous demodulation using a $1\text{-}\mu\text{m}$ triangle-wave modulation of the fine (PZT) stage of the delay line; during one sweep of the PZT the detected photons are grouped into four bins from which the amplitude and phase of the fringe are estimated.⁷ Other optimal filters are under consideration for DS3 fringe searching.¹³ Fringe search time is a function of source magnitude, source visibility, delay uncertainty, and instrument visibility. After detection the fringe is tracked (closed-loop stabilized) by feeding back the fringe position (phase) to the optical delay line. The fringe phase ϕ , estimated using the 4-bin demodulation approach, has the variance¹⁴

$$\sigma_{\phi}^2 = \frac{\pi^2}{4NV^2} \quad (1)$$

where N is the number of detected photons in each coherent integration time, and V is the total instrument visibility,

$$V = V_S V_I \quad (2)$$

the product of the source visibility V_S and the instrument visibility V_I . Source visibilities are equal to 1 for an unresolved target and drop to zero as the target becomes resolved. The instrument visibility V_I accounts for optical inefficiencies and other effects within the instrument and takes on a value between zero and 1; for DS3 we expect V_I to be ~ 0.65 . The fringe phase must be estimated to $\lambda/120$ rms—equivalently 0.05 rad or 5 nm—for sufficient tracking stability. In Eq. 1 the variance of the estimated phase varies inversely with NV^2 : the phase estimate improves with increased number of photons N (greater collecting area, longer integration times) or increased instrument visibility V_I , but is poorer for source visibilities V_S that are near zero. For low source visibility, longer integration times are required for greater N to preserve an accurate phase estimate.

Measure fringe visibility: With the fringe phase actively stabilized, photons can be integrated nearly indefinitely on a CCD detector in many spectral channels to produce estimates of fringe visibility as a function of wavelength. To estimate source fringe visibilities in each spectral channel to 1% of unit visibility, the uncertainties must be considered in both the total visibility measurement V and in the stability of the instrument visibility V_I at each wavelength. A total visibility measurement with uncertainty below 1% may require many seconds or minutes if the source visibility itself is low. The variance of the V^2 estimator using the 4-bin method is¹⁴

$$\sigma_{V^2}^2 = \frac{\pi^4}{4M} \left[\frac{1}{N^2} + \frac{4}{\pi^2} \frac{V^2}{N} \right] \quad (3)$$

Where M is the number of frames, and N is the number of detected photons in each spectral channel and V is the total visibility. Eq. 3 indicates that with sufficient number of photons N an estimate of fringe visibility can be made even when the source visibility is near zero. Furthermore, when source visibilities V_S are nonzero, changes in the instrument visibility V_I will impact the V^2 estimator variance. The uncertainty of the instrument visibility V_I must be maintained to better than 1% between calibrations on bright point sources.

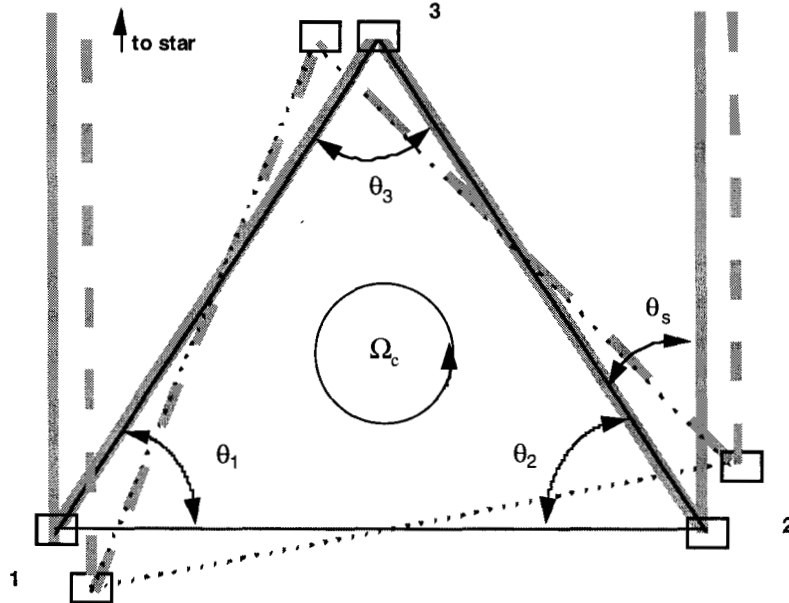


Figure 4: Geometry for delay and delay rate. An in-plane constellation rotation affects interferometer delay.

2.4 Instrument visibility

The instrument visibility is a function of static wavefront figure, relative pathlength stability (phasing), aperture pointing, and intensity matching in each arm of the interferometer.¹⁵ Tolerances must be held in each of these areas to meet the design target of $V_I = 0.65$. For a static wavefront, the optics are required to be $\lambda/100$ rms. For phasing stability, the relative pathlengths of the interferometer must be held constant to a small fraction of a wavelength: The delay line must induce less than $\lambda/60$, or 10-nm rms pathlength jitter, and the metrology resolution must be 5 nm per leg for delay line servo control. In fringe-tracking mode, the fringe phase estimator of Eq. 1 must provide $\lambda/120$ knowledge accuracy, or 5 nm rms, of fringe position for feedback to the optical delay line. Aperture pointing must be maintained to $(0.1\lambda)/d$ rms, or 0.1 arcsec, such that the wavefront tilts of the two combined beams at the beamsplitter are nearly parallel. The starlight angle tracker resolution must be 0.1 arcsec, siderostat angle encoders must be 0.05 arcsec or better, and jitter in the entire optical path—at any frequency above the ~ 10 Hz pointing loops—must also be below 0.1 arcsec rms. Finally, intensity matching requires that the beamsplitter ratio be better than 40:60 and that pupil misalignment at the beamsplitter be less than 3%.

3. INSTRUMENT DESIGN

3.1 Starlight optics

A simplified layout of the DS3 starlight optics is shown in Figures 5 and 6. Starlight is collected by siderostats on two collector spacecraft. The siderostats require a 15° angle of incidence to direct the starlight beam to the combiner spacecraft. The aperture beam diameter is 12 cm and the siderostat flats have dimensions approximately 12×13 cm. A 3-cm central hole accommodates the metrology steering mirror, also a steered flat.

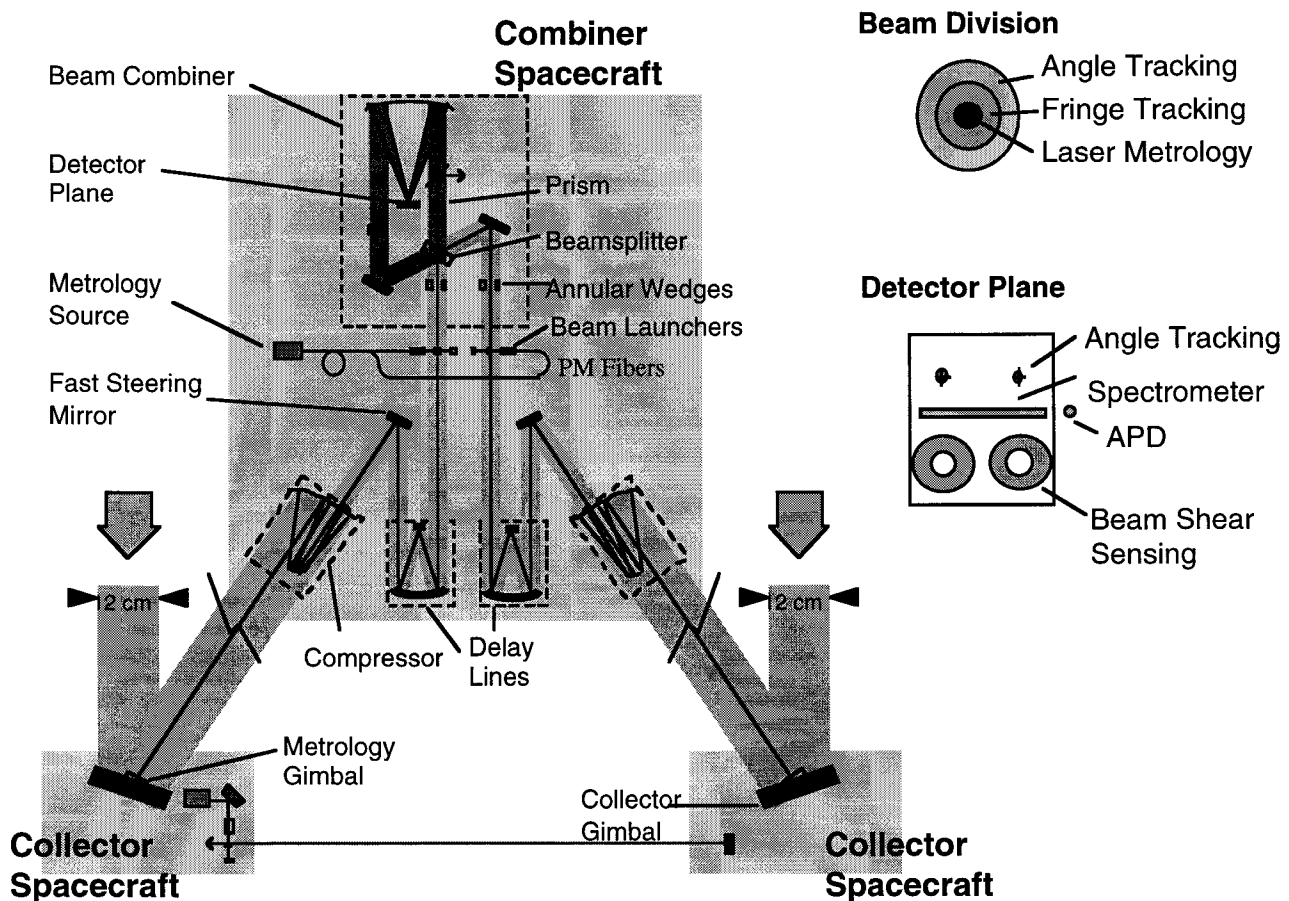


Figure 5: Layout for starlight optics and metrology.

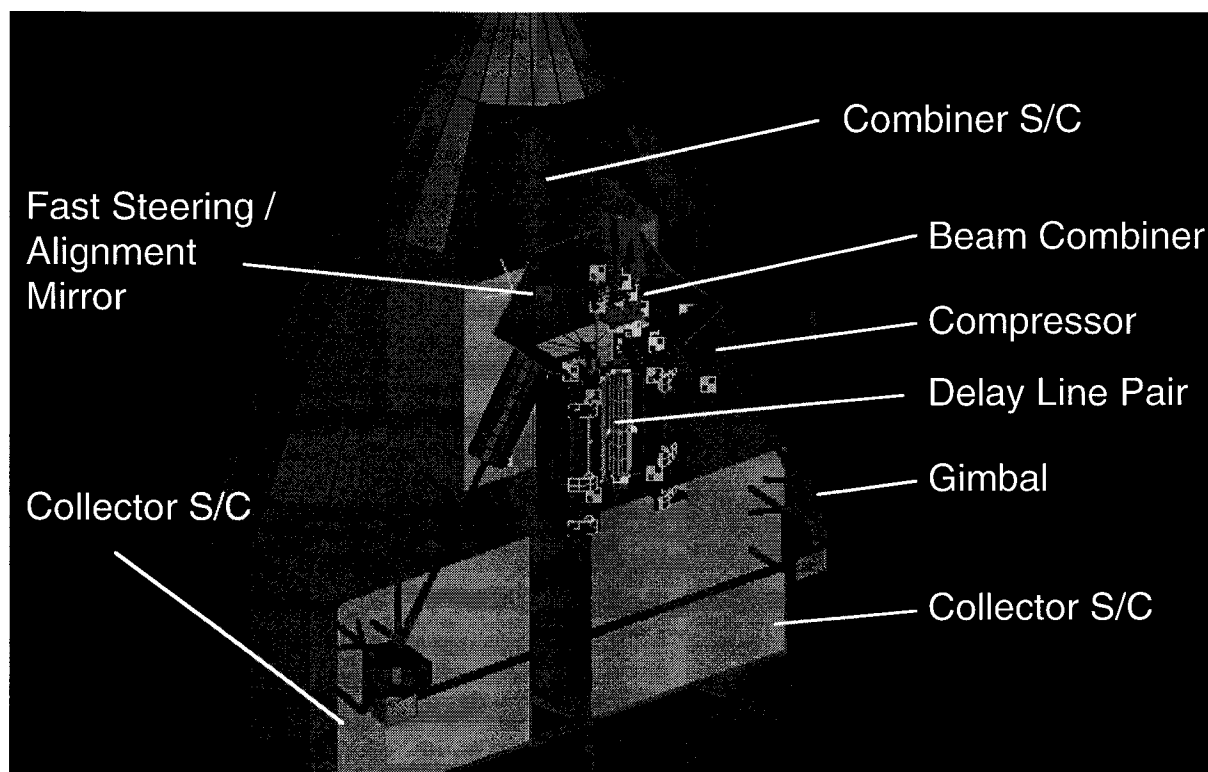


Figure 6: Packaging of DS3 cluster in Delta launch shroud.

The siderostats are articulated in two axes over a range of a few arcmin with a resolution of 50 masec. This resolution corresponds to a 0.5-mm beam centration step size at the receiving optics on the combiner spacecraft, allowing for the angle doubling after reflection and a 1-km distance. The siderostat range overbounds the uncertainty in the formation flying control of relative spacecraft angles and in the attitude control deadband of the collector spacecraft.

Light from the collector siderostat enters the beam combiner at an unobscured afocal compressor. The compression ratio is a factor of 4, so the incoming 12-cm diameter beam exits as a compressed beam with 3-cm diameter. The compressor employs Gregorian optics to provide an internal focus where a field stop will be used to reject off-axis light, a feature that is important when viewing a siderostat adjacent to sunlit spacecraft at 1-km distances, even if the spacecraft is carefully shaded and baffled. The field stop aperture also provides a convenient location for an acquisition camera, which may view a reflective substrate concentric with the field stop aperture.

After the compressor the compressed beam reflects off a fast steering mirror (FSM) used primarily to correct the outgoing laser metrology beam; the FSM may also provide some correction to starlight for disturbances local to the combiner spacecraft. After reflection from the FSM, the beam enters a three-stage optical delay line.^{16, 17} This delay line consists of an $f/5$ cat's-eye parabola with a 9-cm aperture, mounted on a trolley system. The coarse adjustment (0.1 mm to 30 cm) is provided by the trolley, a medium stage (a few μm to a few mm) by voice-coil actuation of the primary mirror cell, and a fine stage (a few nm to a few μm) by a piezoelectric flat at the Newtonian focus of the primary. Both arms of the interferometer have identical delay line optics, though only one delay line need be used for active control.

The compressed beam exits the delay line and enters the beam combiner where it meets the other compressed starlight beam at a beamsplitter. The output of the beamsplitter are two equivalent paths of combined light, indicated in Figure 5 by a darker shade, which are each brought to different regions of the focal plane by a parabolic mirror telescope. In one combined path, the light is imaged to a single-pixel photon-counting detector which is used to track the white-light fringe. In the second path, a dispersive prism provides a spectrally broadened signal that will be used to estimate fringe visibility as a function of wavelength while the fringe is stabilized with the photon-counting detector. Fringe tracking will be performed by modulating the delay line and synchronously estimating the fringe phase, which provides an error signal for delay-line

pathlength control. Interference of the two starlight paths is accomplished at the beamsplitter; detection of the interference is performed at the focal plane.

In fact, not all of the 3-cm starlight beam diameter is used for fringe detection. Consider the cross section of the compressed beam illustrated in Figure 5. The 3 cm beam is divided into three regions: the inner 5-mm is reserved for metrology, and the outer 0.5-cm annulus is used for angle and shear measurements. Only the remaining 2-cm annular is used for starlight fringe detection.

Just prior to the beamsplitter, an annular wedge strips off the outer 5-mm annulus of light in each beam and deflects its angle slightly. These annular pupils from each starlight leg are focused by the parabola into the upper left and right quadrants of the CCD detector as illustrated in Figure 5. The focused star images provide the star-tracking error signal to the siderostat control system. The imaging telescope provides a plate scale on the order of 0.5 arcsec per pixel, and the centroids of the star images can be determined to about 5% of this value, or 25 masec. A second set of these annular beams is provided by the second output path of the beamsplitter, and are offset to the lower left and right quadrants of the CCD. The light is defocused to provide a pupil centration (beam shear) error signal at the image plane.

3.2 Starlight detectors

The focal plane detectors in the combiner imager have three functions: (1) star and beam tracking, (2) white light fringe tracking, and (3) fringe spectral measurements.

Star and beam tracking: A fast-frame CCD is used for the star tracking and beam shear detection. The present baseline is the EEV CCD39, an 80×80 -pixel frame transfer device which can achieve read noise performance of < 5 electrons at 1000 frames per second read rate. The device provides a full-well of 300,000 electrons, and 90% quantum efficiency at 500 nm, with a usable spectral range of 200 to 1100 nm. For DS3, we do not plan to use the range below 350 nm.

White light fringe tracking: For white light fringe tracking, we require a device with quantum efficiency comparable to the CCD, but with photon-counting capabilities to avoid the read-noise floor of the CCD. Its dark current must also be extremely low. The detector of choice is the EG&G Single Photon Counting Module (SPCM), an avalanche photodiode-based device that uses an active quenching circuit to provide very low dead time and dark counts. The dark count rates available in off-the-shelf devices are as low as 10 counts/s, with quantum efficiency as high as 80% at 600 nm. The usable spectral range is well matched to the CCD at 350 to 1100 nm.

Fringe spectrometer: Currently we have baselined a second EEV CCD39 for the fringe spectrometer, which would thus provide 80 spectral channels across its width. Because we intend to integrate for much longer times to improve fringe SNR while the fringe tracker stabilizes the fringe, readout noise as low as 3 electrons per pixel is expected. Because we are using only a few lines of this device, it may be preferable to use the remaining portion of the array for the beam shear images, which generally do not need to be read out as quickly as the star tracker images.

3.3 Metrology subsystem

The DS3 metrology system is designed to measure delay jitter, total delay, and delay rate, requiring both linear and angular metrology between spacecraft.¹⁷ Figure 5 illustrates elements of the linear metrology implementation: One metrology source on the combiner spacecraft feeds two heterodyne interferometer gauges that independently measure pathlength changes in the two combiner-collector starlight paths, and a second metrology source on one of the collector spacecraft feeds another gauge to measure distance changes between the two collector spacecraft. Each gauge consists of the following fiber-coupled components: a 1.3- μ m laser source, frequency shifters, a beam launcher, and phase detection/control electronics.¹⁸

In each starlight leg, the metrology is injected near the combiner beamsplitter as a 50-mW, 5-mm diameter beam concentric with the 3-cm compressed starlight beam. The metrology follows the same path as the starlight from a fiducial near the combiner beamsplitter out to a 2-cm steered at the center of each siderostat; changes in this distance are measured by the linear metrology. The diameter of the metrology beam is increased from 5 mm to 2 cm by the 4:1 compressor, which acts as an expander; diffraction leads to a 12-cm Gaussian beam diameter at a collector located at 1 km distance. The total round-trip power loss is -25 dB, meaning that only 0.3% of the launched power returns to the heterodyne gauge. High power loss in the range-related signal in addition to polarization leakage within the source gauge leads to self-interference and a loss of metrology accuracy. Frequency modulation of the source is proposed to avoid problems from self-interference.

Figure 7 illustrates components of the interspacecraft angular metrology. Metrology acquisition between spacecraft is performed by steering the outgoing beams from the combiner using the fast steering mirrors over the ± 1 -arcmin field afforded by the aperture stop in the compressor; any larger range would require an attitude change of the combiner spacecraft. At the collector spacecraft the metrology beam is detected by an array of intensity gradient detectors around the perimeter of the collector siderostat, which are used in a 10-to-50 Hz feedback loop to the combiner fast steering mirror to center the metrology on the siderostat to 0.25 mm, or 50 msec at 1 km. On the return leg to the combiner, the 2-cm metrology mirror is articulated until it has been centered on the combiner to the same accuracy. Because of the low power of the returned signal, phase gradient detectors will instead be used at the combiner. Closed-loop control, using interspacecraft communication in the loop, is maintained between each steering mirror and the metrology detectors on the opposing spacecraft. Each interspacecraft metrology leg is aligned this way.

Once locked by a closed pointing loop, angle encoders, accurate to 50 msec, in each of the steering mirrors reference the metrology line of sight to the local instrument optical bench and establish constellation relative angle knowledge to 50 msec.

Delay and delay rate estimation: Delay estimation is accomplished by using a total of five angle measurements: four from the angle encoders on the metrology steering mirrors, and one from a siderostat gimbal angle encoder after the starlight from that siderostat has been centered on the CCD angle tracker. All angles are in the plane of the constellation; out-of-plane angle changes do not affect the interferometer delay to first order. The starlight gimbal angle is required to reference the constellation geometry to the inertial line of sight to the target.

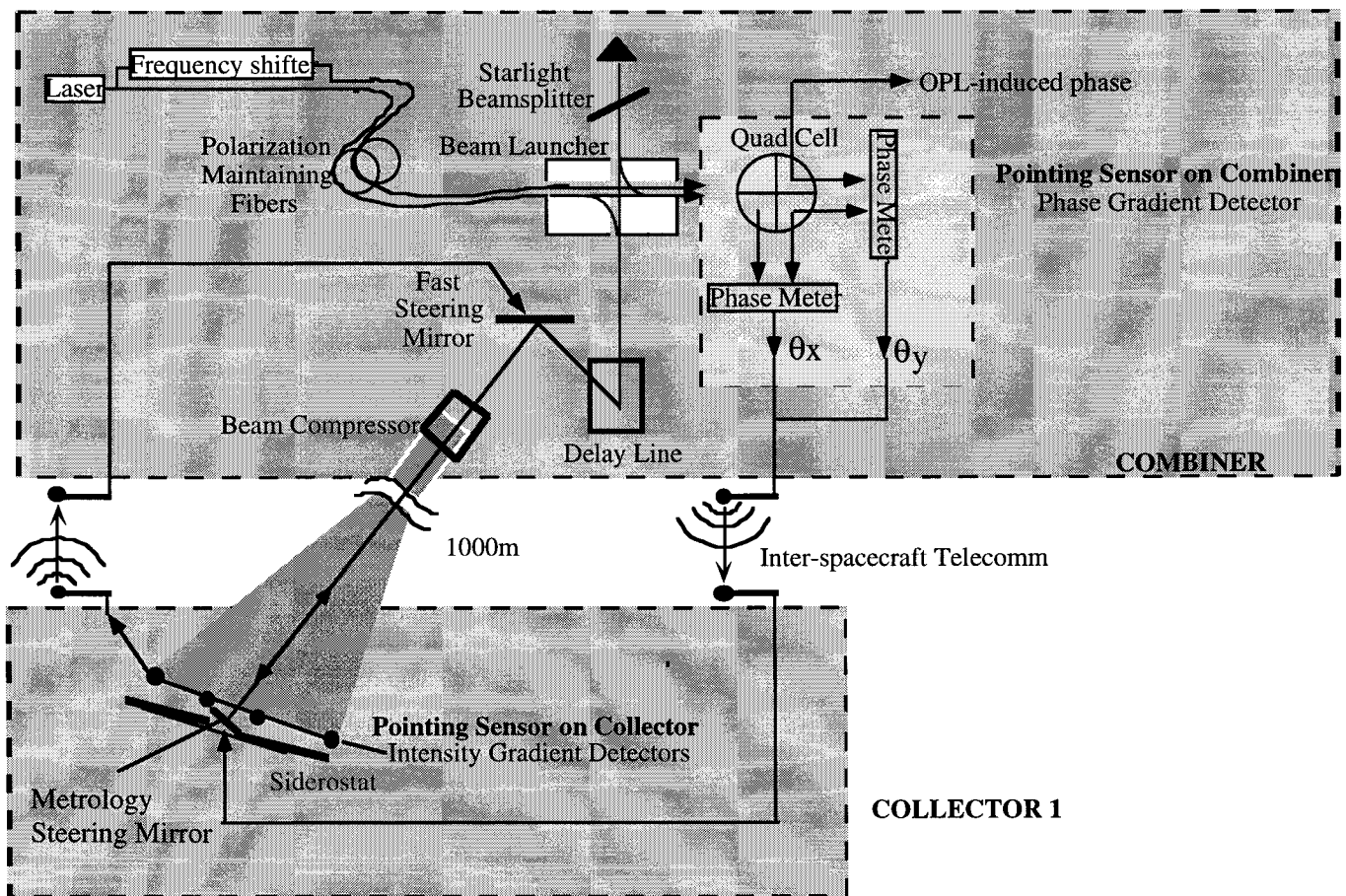


Figure 7: Details of the metrology subsystem.

The constellation delay rate could be determined by the time rate of change of this delay estimate. However, the use of linear metrology to measure changes in the relative spacecraft separations reduces the angular measurements needed for a delay rate estimate to the difference between the starlight and metrology angle encoders on only one of the collector spacecraft. The delay rate estimates for dim stars require measurement of these angles over a period of ~ 600 s, and require a resolution and stability (over 600 s) to 50 msec.

An alternative method for estimating delay rate has been considered but is not currently baselined in DS3 due to cost and technical readiness. The concept, termed the Kilometric Optical Gyro, or KOG, is based on setting up a Sagnac interferometer in the DS3 constellation. Two counterrotating metrology beams are interfered, and the resulting phase difference is proportional to both the enclosed area of the triangle and the rotation rate of the constellation about an axis normal to the constellation plane. Although more complex to implement, the KOG would provide a more accurate delay rate estimate than the method based on time evolution of starlight and metrology gimbal angles.

4. SUMMARY

We have presented a description of the DS3 mission and of the instrument payload—a Michelson interferometer with collecting and combining optics distributed among three spacecraft flying in a 1-km formation. Fundamental instrument requirements were presented for baseline, limiting magnitude, calibration accuracy of visibility amplitude, and degree of aperture plane coverage for astrophysical targets. A description was provided for the steps that the instrument must perform at each baseline orientation—metrology acquisition, estimation of delay and delay rate, and the search, tracking and measurement of stellar fringes—and requirements for the starlight and metrology subsystems were derived. Engineering implementations of the starlight and metrology subsystems were presented. During the remainder of the preproject phase, requirements and engineering implementations will be reviewed and further defined.

5. ACKNOWLEDGMENTS

The work described in this paper was carried out by the Jet Propulsion Laboratory, California Institute of Technology, under contract with the National Aeronautics and Space Administration.

6. REFERENCES

1. Naderi, F. M., "NASA's ORIGINS Program," *SPIE International Symposium on Astronomical Telescopes and Instrumentation*, Paper no. 3350-125, March 1998.
2. Shao, M., "Space Interferometry Mission," *SPIE International Symposium on Astronomical Telescopes and Instrumentation*, Paper no. 3350-01, March 1998.
3. Purcell, G., Kuang, D., Lichten, S., et al., "Autonomous Formation Flyer (AFF) Sensor Technology Development," *21st Annual AAS Guidance and Control Conference*, February 1998, AAS 98-062.
4. Blandino, J. J., Cassady, R. J., and Peterson, T. T., "Pulsed Plasma Thrusters for the New Millennium Interferometer (DS-3) Mission," *25th International Electric Propulsion Conference*, August 1997, Cleveland, OH, IEPC 97-192.
5. Lau, K., Lichten, S., Young, L., and Haines, B., "An Innovative Deep Space Application of GPS Technology for Formation Flying Spacecraft," *AIAA GN&C Conference*, July 1996, AIAA 96-3819.
6. Lau, et al., "Separated Spacecraft Formation Flying Control Technologies for the New Millennium Deep Space 3 Mission," *SPIE International Symposium on Astronomical Telescopes and Instrumentation*, Paper no. 3350-82, March 1998.
7. Shao, M., Colavita, M. M., Hines, B. E., et al., "The Mark III Stellar Interferometer," *Astron. Astrophys.* 193, 357-371 (1988).
8. Shao, M., and Colavita, M. M., "Long Baseline Optical and Infrared Stellar Interferometry," *Ann. Rev. Astron. Astrophys.* 1992. 30: 457-98
9. Goodman, J., *Statistical Optics*. New York: John Wiley & Sons, 1985, pp. 331-347.
10. Linfield, R. P., and Gorham, P. W., "Science Capabilities of the DS3 Mission," *SPIE International Symposium on Astronomical Telescopes and Instrumentation*, Paper no. 3350-10, March 1998.

11. Linfield, R., "Number of Sources DS3 Can Observe, as a Function of Spacecraft Power," JPL Internal IOM 335.1-97-014, May 16, 1997.
12. Linfield, R., "DS3 Delay and Delay Rate Estimation. Revised Algorithm Without a Starlight Shear Sensor," JPL Internal IOM 335.1-98-001, Jan 29, 1998.
13. Gorham, P. W., and Linfield, R. P., "Optimal Filter Approach to Photon-Limited White Light Fringe Detection and Delay Rate Estimation in an Optical Interferometer," *SPIE International Symposium on Astronomical Telescopes and Instrumentation*, Paper no. 3350-72, March 1998.
14. Colavita, M. M., "Atmospheric Limitations of a Two-Color Astrometric Interferometer," Doctoral thesis dissertation, Department of Electrical Engineering, Massachusetts Institute of Technology, 1985, pp. 217-277.
15. McGuire, J., and Colavita, M., "New Millennium Interferometer: Preliminary Design Rev. A," JPL Internal IOM, January 22, 1996.
16. Calvet, R., Joffe, B., Moore, D. M., et al., "Enabling Concepts for a Flight Qualifiable Optical Delay Line," *SPIE International Symposium on Astronomical Telescopes and Instrumentation*, Paper no. 3350-64, March 1998.
17. Grogan, R. L., Blackwood, G. H., and Calvet, R. J., "Optical Delay Line Nanometer Level Pathlength Control Law Design for Space-Based Interferometry," *SPIE International Symposium on Astronomical Telescopes and Instrumentation*, Paper no. 3350-62, March 1998.
18. Dubovitsky, S., et al., "Deep Space 3 Metrology System," *SPIE International Symposium on Astronomical Telescopes and Instrumentation*, Paper no. 3350-11, March 1998.
19. Dubovitsky, S., Seidel, D. J., Liu, D. T., and Gutierrez, R. C., "Metrology Source for High Resolution Heterodyne Interferometer Laser Gauges," *SPIE International Symposium on Astronomical Telescopes and Instrumentation*, Paper no. 3350-50, March 1998.